Earthquake Engineering, Tenth World Conference © 1992 Balkema, Rotterdam. ISBN 90 5410 060 5

High-strength concrete beam-column joints

S.W.Shin & K.S.Lee
Han Yang University, Seoul, Korea

S.K.Ghosh
Portland Cement Association, Skokie, Ill., USA

ABSTRACT: American Concrete Institute (ACI) - American Society of Civil Engineers (ASCE) Joint Committee 352 on Joints and Connections in Monolithic Concrete Structures (1985) has made several recommendations concerning the design of joints that are part of the primary system for resisting seismic lateral loads. The recommendations are based on tests of normal-strength concrete connections with compressive strength f'_c ranging between 3500 and 5500 psi (24 and 38 MPa). This experimental investigation was undertaken to check the validity of the recommendations for high-strength concrete beam-column joints.

1 OBJECT AND SCOPE

ACI-ASCE 352 (1985) recommends that for joints which are part of the primary system for resisting seismic lateral loads, the sum of the nominal moment-strengths of the column sections above and below the joint (ΣM_c), calculated using the axial load which gives the minimum column-moment strength, should not be less than 1.4 times the sum of the nominal moment strengths of the beam sections at the joint (ΣM_g). It may be noted that in the ACI 318 (1989) "Building Code Requirements for Reinforcement Concrete," the minimum required flexural strength ratio $\Sigma M_c/\Sigma M_g$ is 1.2, instead of 1.4. ACI-ASCE 352 (1985) further recommends that where rectangular hoop and crosstie reinforcement is used to confine the concrete within a joint, the center-to-center spacing between layers of transverse reinforcement should not exceed the least of one-quarter of the minimum column dimension (h_c), six times the diameter of the longitudinal bars to be restrained, or 6 in. (150 mm). It may again be noted that in ACI 318 (1989), the maximum spacing of transverse reinforcement is restricted to the smaller of $h_c/4$ or 4 in. (100 mm).

In order to check the validity of the above recommendations for high-strength concrete beam-column joints, one normal-strength and ten high-strength concrete half-scale beam-column joint specimens were constructed and tested. One of the high-strength specimens was tested under monotic loading, all others were tested under reversed cyclic loading. According to the classification in the ACI-ASCE 352 (1985) recommendations, the configuration of the specimens qualified them as corner connections. The variables investigated were:

1. The concrete compressive strength (f'_c = 4380 and 11,380 psi or 30.2 and 78.5 MPa),
2. Number of confining hoops within the joint core (3,2,1 and 0; corresponding spacing = $h_c/4$, $h_c/3$, $h_c/2$, and infinity, respectively),
3. Type of loading (cyclic, monotonic),
4. Column-to-beam flexural strength ratio (M_r = $\Sigma M_c/\Sigma M_g$ = 1.4, 1.6, 1.8, and 2.0), and
5. Number of bent-up bars within the joint core (1 and 2).

2 MATERIALS, SPECIMENS, TEST SETUP AND PROCEDURE

The column in each specimen was 6x6 in. (150x150 mm) in cross section and 32 in. (800 mm) long. The beam was 4-4/5x8 in. (120x200 mm) in cross-section, and 39 in. (975 mm) long. Details of the specimens are given in Tables 1 and 2 and in Figure 1.

The cement used was Type 2 portland cement, fine aggregate was natural Han River sand with a fineness modulus of 3.0, coarse aggregate was crushed limestone with a maximum size of 1/2 in. (13 mm), and superplasticizer was Super-20 (Grace Co., Napthalene series). In all specimens, deformed steel having a specified yield strength of 56,900 psi (392 MPa) was used for longitudinal reinforcement in the column and the beam. Confinement reinforcement was made of deformed steel having a specified yield strength of 34,100 psi (235 MPa). The spacing of confinement reinforcement was 2 in. (50 mm) in the columns and the beams.

Each specimen was cast horizontally with 1 batch of concrete which was also used to cast the accompanying cylinders. The beam-column joint specimens were kept in their forms under atmospheric conditions for 2 days, and were moist-cured in water at a temperature of 77-86°F (25-30°C) following the removal of forms. They were then stored in the laboratory until testing.

Figure 2 schematically shows the test setup. The column of each specimen was kept under a constant axial load equal to 40 percent of the balanced axial load. The vertical load on the beam was applied at 36 in. (980 mm) from the column face. All reversed cyclic loading tests were run under displacement control. The displacement sequence applied at the end of each beam is illustrated in Figure 3. Δ_y in Figure 3 is the vertical beam displacement at the point of loading, corresponding to yielding of the longitudinal beam reinforcement at the

Table 1. Description of test specimens

Specimens	f'_c psi (MPa)	Loading Type*	Number of Hoops in Core	M_r ($\Sigma M_c/\Sigma M_g$)	Number of Bent-up Bars in Core
NJC3-R0	4380 (30.2)	C	3	1.4	0
HJM3-R0	11,380 (78.5)	M	3	1.4	0
HJC3-R0	"	C	3	1.4	0
HJC2-R0	"	C	2	1.4	0
HJC1-R0	"	C	1	1.4	0
HJC0-R0	"	C	0	1.4	0
HJC3-R1	"	C	3	1.8	0
HJC3-R2**	"	C	3	1.8	0
HJC3-R3	"	C	3	2.0	0
HJC3-R0-B1	"	C	3	1.4	2
HJC3-R0-B2	"	C	3	1.4	1

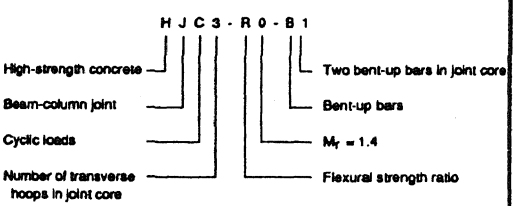

*C—Cyclic load, M—Monotonic load
**HJC3-R2 failed prematurely

Table 2. Description and load capacities of test specimens

Specimen	Column		Beams		Loading Pattern	P_{max} kips (kN)
	Section in. (mm)	Reinforcement	Section in. (mm)	Reinforcement		
NJC3-R0	6 × 6 (150 × 150)	8 #3 (10mm dia.)	4½ × 8 (120 × 120)	4 #4 (13mm dia.) 2 #3 (10mm dia.)	C	8.82 (39.23)
HJM3-R0	"	"	"	6 #4 (13mm dia.)	M	13.78 (61.29)
HJC3-R0	"	"	"	"	C	10.03 (44.62)
HJC2-R0	"	"	"	"	C	12.68 (56.39)
HJC1-R0	"	"	"	"	C	10.36 (46.09)
HJC0-R0	"	"	"	"	C	9.58 (42.66)
HJC3-R1	"	"	"	4 #4 (13mm dia.) 2 #3 (10mm dia.)	C	10.77 (48.05)
HJC3-R2		"	"	4 #3 (10mm dia.) 2 #4 (13mm dia.)	C	"
HJC3-R3	"	"	"	6 #3 (10mm dia.)	C	6.81 (30.40)
HJC3-R0-B1	"	"	"	6 #4 (13mm dia.)	C	7.72 (34.32)
HJC3-R0-B2	"	"	"	"	C	10.03 (44.62)

*HJC3-R2 failed prematurely

column face. In the case of the specimen resisting monotonic loads, the test was conducted under load control until one-third of the expected maximum load was attained; a switch was made to displacement control thereafter.

3 FAILURE PATTERN

In HJM3-R0, which resisted monotonic loading, a few hairline flexural cracks formed in the beam between the column face and a section one effective beam depth away from the column face. Such cracks propagated into the joint core and opened the face of the beam-column joint in the tension region. As the crack at the beam-column joint face opened widely in the tension region, the test was concluded.

In all other specimens, initial flexural cracks formed in the beam between the column face and a section one-quarter of the beam depth away from the column face. Minor diagonal cracks formed within the joint core at load stage 2 (cycles 4-6), except in specimens HJC3-R3 (M_r = 2.0), and HJC3-R0-B1 (two bent-up bars within the joint core). Obvious diagonal cracks formed within the joint core at load stage 3 (cycles 7-9) in all specimens except those having $M_r > 1.4$ and those having bent-up bars within the joint core.

In specimens designed with less joint confinement than recommended by ACI-ASCE 352 (1985) (HJC2-R0, HJC1-R0, HJC0-R0), the cracks within the joint core propagated up and down the column, beyond the joint core panel zone, at load stage 4 (cycles 10-12). At advanced deformation stages, the cover concrete in the joint regions of these specimens was fully destroyed, and the transverse reinforcement exposed; the longitudinal column reinforcement also buckled.

In the normal-strength concrete specimen NJC3-R0, many hairline flexural cracks formed uniformly along the beam at low displacement stages; failure occurred in the beam region between the column face and a section one-quarter of the beam depth away from the column face. In the corresponding high-strength concrete specimen HJC3-R0, wide cracks were concentrated at the beam-column joint face. Visually and otherwise, damage to the high-strength specimen was more severe than damage to the normal-strength specimen. Figure 4 graphically shows the effects of the other test variables on the failure mode.

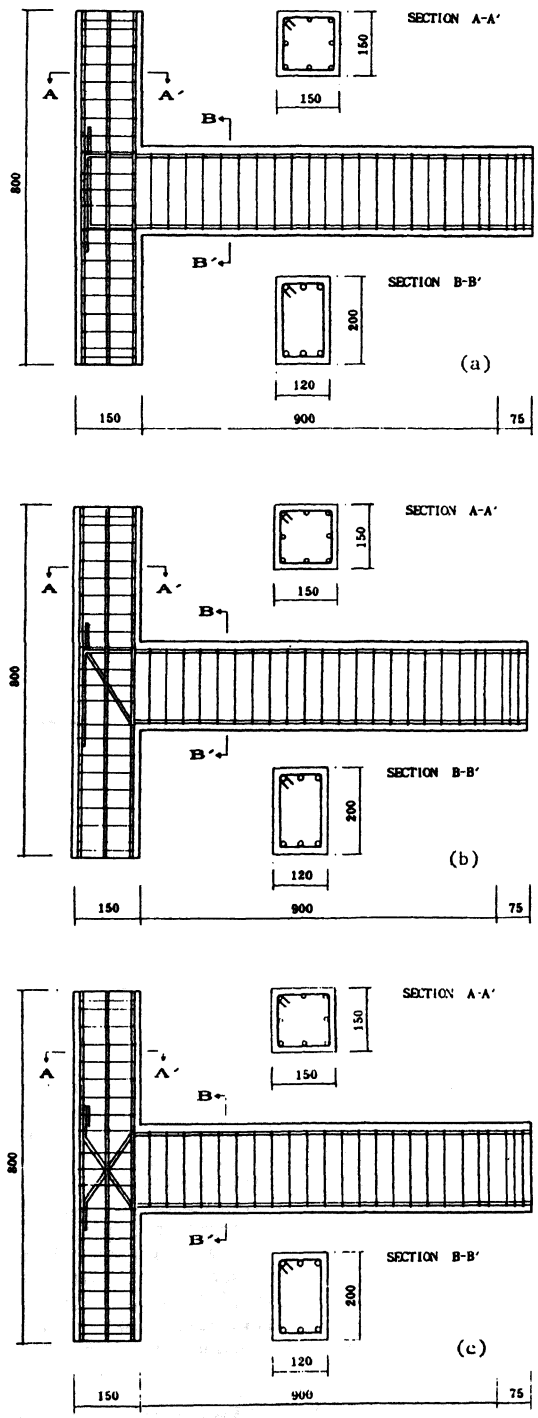

Figure 1. Specimen reinforcing details (a) all specimens except HJC3-R0-B1, HJC3-R0-B2, (b) HJC3-R0-B2, (c) HJC3-R0-B1

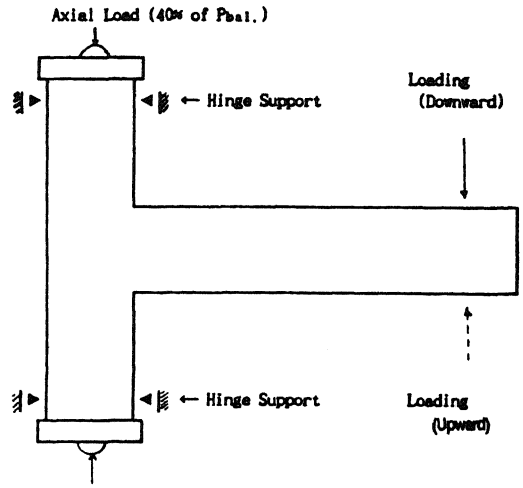

Figure 2. Test setup

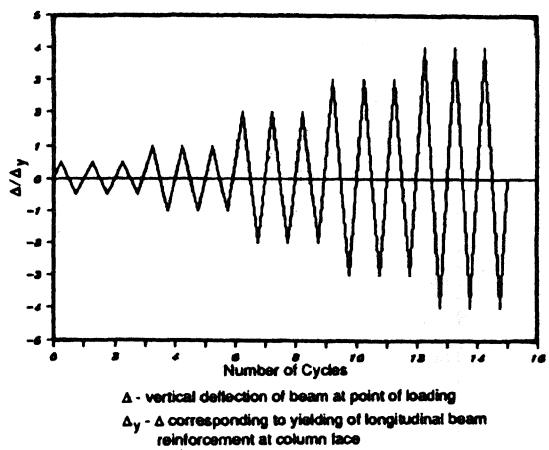

Figure 3. Deformation sequence for reversed cyclic loading tests

4 HYSTERETIC LOAD-DISPLACEMENT BEHAVIOR

A sample hysteretic load-displacement curve, for specimen HJC3-R0, is illustrated in Figure 5. Generally, load resisting capacities increased until load stage 3 (cycles 7-9). Beyond that, the load capacities declined differently, depending on the test parameters. A comparison between the hysteresis loops for NJC3-R0 (f'_c = 30.2 MPa) and HJC3-R0 (f'_c = 78.5 MPa) showed distinctly pinched hysteresis loops for HJC3-R0, probably because failure of HJC3-R0 was largely concentrated at the beam-column joint face. Bond strength of longitudinal beam reinforcement deteriorated because of shear failure at the joint face.

The amount of transverse confinement reinforcement within the joint core had little effect on hysteretic

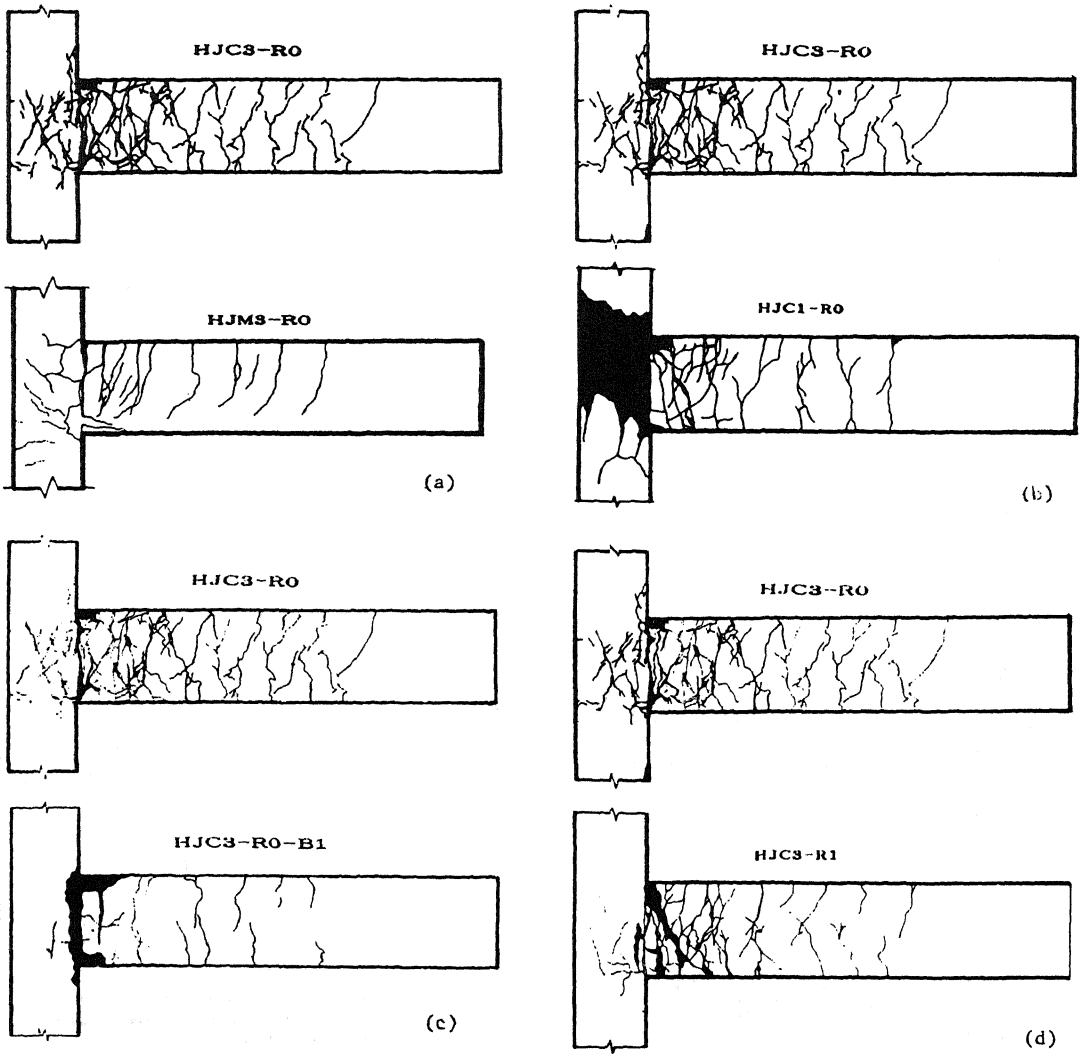

Figure 4. Failure modes of specimens with (a) different loading patterns, (b) different confinement reinforcement, (c) different bent-up bars, and (d) different flexural strength ratios

behavior of the specimens. However, at advanced deformation stages, the load resisting capacity of HJC3-R0, designed with a confinement reinforcement spacing of $h_c/4$ according to ACI-ASCE 352 (1985) recommendations, decreased less than those of HJC2-R0, HJC1-R0 and HJC0-R0.

In HJM3-R0 subject to monotonic loading, initial diagonal crack within the joint core formed at 35.8 kN; in HJC3-R0 subject to reversed cyclic loading, it formed at 28.4 kN. The maximum loads for HJM3-R0 and HJC3-R0 were 61.3 kN and 44.6 kN, respectively. The ratios of diagonal cracking loads and maximum loads between HJM3-R0 and HJC3-R0 are 1.26 and 1.37, respectively. The differences are due to the loss of bond strength and deterioration of aggregate interlock caused by cyclic loading.

Specimen HJC3-R0-B1, with two bent-up bars within the joint core, exhibited distinctly pinched hysteresis loops. The hysteresis loops were less pinched for HJC3-R0-B2, with one bent-up bar within the joint core. However, the hysteresis loops were more pinched for HJC3-R0-B2 than for HJC3-R0, with no bent-up bars. In HJC3-R0, damage was spread over the beam and the beam-column joint core; in HJC3-R0-B1, damage was concentrated between the beam-column joint face and the nearest layer of longitudinal column reinforcement.

5 ENERGY DISSIPATION CAPACITY

Energy dissipation capacity, as defined in Figure 6, is plotted in Figures 7, 8 and 9 for specimens with different confinement reinforcements within the joint core, different bent-up bars within the joint core, and different beam-column flexural strength ratios, respectively. In all these figures, the energy dissipation capacities of high-

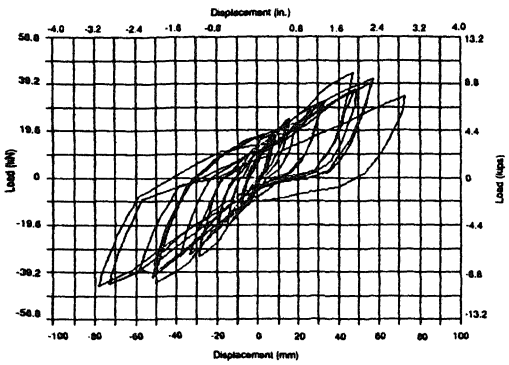

Figure 5. Load-displacement curves for specimen HJC3-R0

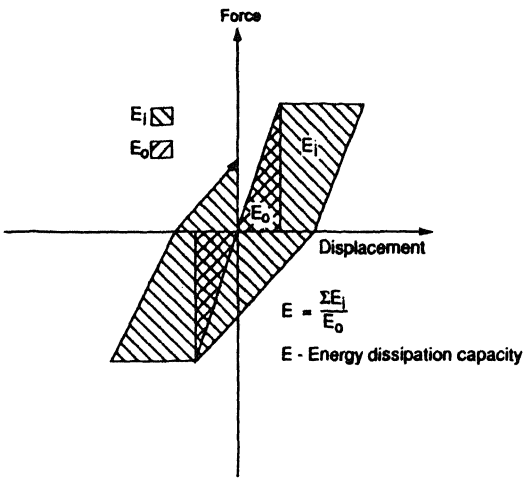

Figure 6. Definition of energy dissipation capacity, as plotted in Figures 7-9

strength concrete specimens should be compared to that of the normal-strength concrete specimen, NJC3-R0. Figure 7 shows that only HJC2-R0 exhibited higher energy dissipation capacity than NJC3-R0. It should be noted, however, that the column of HJC2-R0 was severely damaged through load stages 4 and 5 (cycles 10-15). Figure 8 shows that with the addition of bent-up bars within the joint core, the energy dissipation capacities of high-strength concrete specimens approach that of the comparable normal-strength concrete specimen. Figure 9 shows a definite correlation between energy dissipation capacity and column-beam flexural capacity ratio, and indicates that a ratio of at least 1.6 is needed for the energy dissipation capacity of a high-strength concrete beam-column joint specimen to match that of a comparable normal-strength concrete specimen.

6 CONCLUSIONS

The following conclusions could be drawn on the basis of the test results:

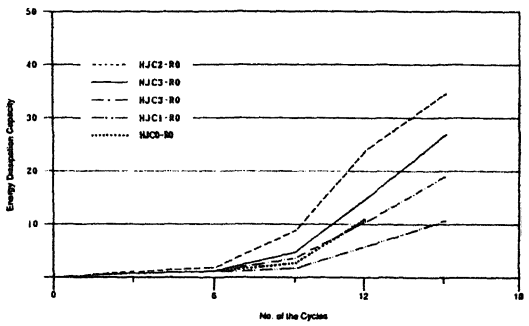

Figure 7. Energy dissipation capacity, as affected by confinement reinforcement within joint

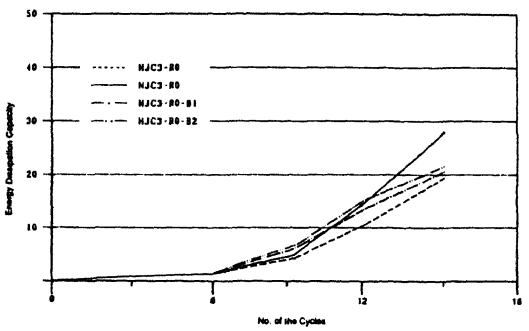

Figure 8. Energy dissipation capacity, as affected by different bent-up bars within joint

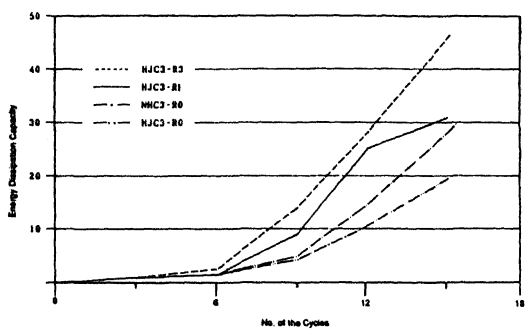

Figure 9. Energy dissipation capacity, as affected by different column-beam flexural strength ratios

1. In high-strength concrete beam-column joints subjected to reversed cyclic loading, combined bending and shear was the final failure mode. Under monotonic loading, the final failure was dominated by bending.
2. In high-strength concrete beam-column joints designed with wider transverse reinforcement spacing than recommended by ACI-ASCE 352 (1985), failure occurred in the beam-column joint core, and extended throughout the panel zone, into the upper and lower columns. Thus the spacing recommendation appears to be valid for high-strength concrete beam-column joints.
3. The behavior of high-strength concrete beam-

column joint specimens with bent-up bars within the joint core was shear dominated; the hysteretic load-displacement loops were severely pinched due to stress concentration at the beam-column joint face. Thus, the use of such bent-up bars should be avoided.

4. The lower limit value of the column-to-beam flexural strength ratio may have to be adjusted from 1.4 to 1.6 for high-strength concrete beam-column joints, if energy dissipation capacity of the joint region is a prime design consideration.

REFERENCES

ACI-ASCE Committee 352.1985. *Recommendations for design of beam-column joints in monolithic reinforced concrete structures*. ACI 352R-85. Detroit: ACI.

ACI Committee 318.1989. *Building Code Requirements for Reinforced Concrete*. ACI 318-89. Detroit: ACI.